Pergamon

Tetrahedron 54 (1998) 12323–12336

TETRAHEDRON

Hydrogen Bonding Effects in the Epoxidation of Propenol with Dioxiranes. A DFT Computational Study.

Mauro Freccero[a], Remo Gandolfi[a], Mirko Sarzi-Amadè[a*], Augusto Rastelli[b].

[a]Dipartimento di Chimica Organica, Università di Pavia, V.le Taramelli 10, 27100 Pavia Italy.
[b]Dipartimento di Chimica, Università di Modena, Via Campi 183, 41100 Modena, Italy.

Received 3 June 1998; revised 22 July 1998; accepted 30 July 1998

Abstract: Potential energy surfaces for the epoxidations of 2-propen-1-ol with dioxirane (DHD) and dimethyldioxirane (DMD) were investigated at the B3LYP/6-31G* level. Seven transition structures (TSs) were located for the reaction of DHD. The four chemically more significant TSs were located also for the reaction of DMD. Geometries and energies of two of them clearly demonstrate that stabilizing hydrogen bonding interactions can be at work and that they involve both the dioxirane oxygens. Calculations indicate that the electron attracting effect of the allylic hydroxy group has a relatively small rate retarding effect. Calculations predict higher reactivity for propenol with respect to propene reaction in gas phase but introduction of electrostatic solvation effects (acetone, Tomasi model) leads to reactivity reversal in substantial agreement with experimental data.

Keywords: Dioxiranes; Epoxidation; Transition states; Hydrogen bonding; Allylic Alcohols

INTRODUCTION

In a few years dioxirane oxidations[1-4] have rapidly grown into one of the most useful oxidation processes and are now firmly placed in the arsenal of organic reactions. In particular they rival the long established peroxyacid epoxidation of olefin owing to their neutral and very mild reaction conditions as well as to comparable or even higher reaction rates.

The reaction rate of olefin epoxidation by dimethyldioxirane[5-8] (DMD) in acetone/water (the protocol more frequently used) benefits both from the medium polarity and from the hydrogen bond donor property of water.[9,10] In fact on passing from reactants to transition state there is a sizable increase in the dipole moment of the system (by *ca.* 2 D in the reaction of DMD with ethene and other simple alkenes) while the electron density transfer from the olefin to DMD (*ca.* 0.3 electrons in the reaction with ethylene, propene and 2-butenes) together with the O----O bond cleavage, with net charge increase on the distal oxygen, sets the stage for intermolecular (and intramolecular)[11-14] hydrogen bonding interactions. Convincing experimental evidence of rate acceleration attributable to intermolecular hydrogen bonding interactions has been reported: for example, passing from pure acetone to acetone/water (36:64) leads to decrease in activation free enthalpy (at 23 °C) by 6.3 kJ mol^{-1} (corresponding to a 14-fold rate enhancement) in the reaction of DMD with p-methoxystyrene.[10]

The problem of intermolecular hydrogen bonding in dioxirane epoxidations (methanol as solvent) has computationally been addressed very recently by Houk, Jorgensen and co-workers with the B3LYP/6-31G* method and Montecarlo simulations.[15] Their results suggest that, at variance with qualitative models in which hydrogen bonding with the distal oxygen is assumed,[13,14] e.g. **A** in Scheme 1, a strong hydrogen bond bridges

0040-4020/98/$ - see front matter
PII: S0040-4020(98)00742-X

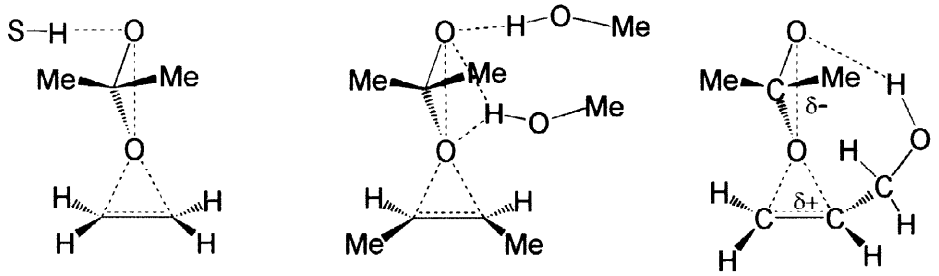

Scheme 1. **A** and **C**: intermolecular (with solvent) and, respectively, intramolecular hydrogen bonding models suggested by experimentalists. **B**: intermolecular hydrogen bonding interactions (methanol as solvent) as suggested by computational data.

the two DMD oxygen atoms while a second molecule of methanol is involved in a further hydrogen bond with the distal DMD oxygen, i.e. **B**.

Intramolecular hydrogen bonding interactions seem to play an important role in controlling facial selectivity of epoxidation of allylic alcohols by DMD. These effects clearly emerge in solvents, such as carbon tetrachloride, which can not act either as hydrogen bond donors or hydrogen bond acceptors. Actually, going from solvents such as acetone or acetone/methanol (10:90) to acetone/carbon tetrachloride mixtures (5:95 and 10:90) adds a significant favor ($\leq$6.3 kJ mol^{-1}) to syn attack in the DMD epoxidation of 2-cyclohexen-1-ol derivatives.[13] Involvement of the sole distal oxygen of the dioxirane moiety is always assumed when qualitative and schematic transition structures are depicted in order to illustrate this effect, e.g. **C** in Scheme 1.

Curci *et al.*[4] questioned the role of intramolecular hydrogen bonding by allylic hydroxy groups as facial selectivity directing factor on the basis of absolute rate epoxidation data. They reasoned that intramolecular hydrogen bonding in the transition state should lead to enhancement in reaction rates of DMD epoxidations of allylic alcohols in comparison to those of the corresponding alkenes. However, they emphasized that, at odds with this conclusion, the opposite is observed experimentally: i.e., on going from 3-methyl-1-pentene and 3,3-dimethyl-1-butene to 3-methyl-1-penten-3-ol and 3-methyl-1-buten-3-ol, respectively, the reaction rate constant of DMD epoxidation halves. Murray *et al.*[12] suggested that the electron withdrawing inductive effect of the hydroxy group retards reaction rate and in allylic alcohols (as well as in homoallylic alcohols) it prevails over possible rate enhancing intramolecular hydrogen bonding effects. They also stressed that in acyclic derivatives the latter factors clearly show them up only when there is a tether of two methylene groups between the double bond and the CH_2OH center (as in 2-methylhex-5-en-2-ol): this kind of tether allows the activated complex to easily assume a conformation in which a very efficient hydrogen bonding interaction between the hydroxy group and the distal oxygen of the dioxirane moiety can be at work.

It is quite clear that, in order to throw light on the structural details of activated complexes (geometries, charge transfer, etc.) suggested by experimentalists to explain their interesting kinetic and diastereoselectivity results in dioxirane epoxidation of unsaturated alcohols, it is necessary to calculate transition structures at good theory level. Fortunately, density functional theory provides us with methods, such as the B3LYP/6-31G* method, which give reliable transition structure geometries for dioxirane epoxidations.[16-18] In contrast these reactions are not treated correctly by HF methods such as the HF/6-31G* method.[19] Moreover, the B3LYP/6-31G* method, taking into account substantial amounts of electron correlation,[20,21] satisfactorily reproduces not only relative reactivity but also absolute reactivity data and it seems to perform definitely better (at least for these reactions) and at lower costs than the simplest post HF method, i.e., the MP2/6-31G* method.[22]

We started to computationally address the problem of intramolecular hydrogen bonding in dioxirane reactions by studying the reaction of DHD with propenol. We were able to find seven TSs for this reaction. Then we passed to the reaction of DMD and located the four (out of seven) chemically more interesting TSs.

In these studies we aimed at precisely defining the geometries of all transition structures and their relative energies in systems in which steric effect are missing as far as possible. In particular we were interested to evaluate whether intramolecular hydrogen bonding can be at work in epoxidation of allylic alcohols and which

oxygen of the dioxirane moiety is involved in this interaction. Moreover we hoped to answer the question whether the energy gain attributable to hydrogen bonding can override the rate retarding electron withdrawing effect of the hydroxy group.

When our study was almost complete, Miaskiewicz *et al.*[23] published their investigation of the epoxidation of 3-methyl-2-butenol with DMD by the B3LYP/6-31G* method. Only two TSs were located by these authors. Our study, while substantially confirming their results, offers a much more detailed and complete description of the dioxirane epoxidation of allylic alcohols (in a context free from steric complications).

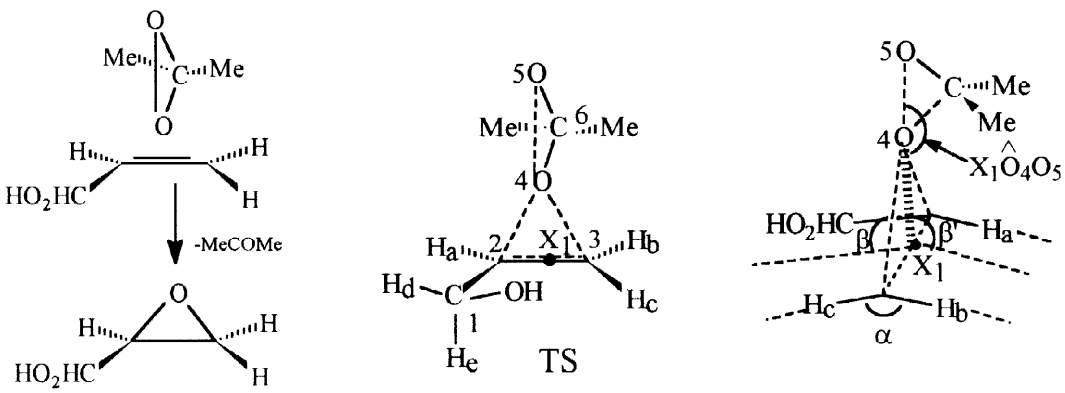

Scheme 2.

COMPUTATIONAL METHODS

Electronic energies (Table 1, 2 and 4) and geometries (Table 1, 3 and 5) of the reactants as well as of the transition structures [TSs] were calculated with density functional theory (DFT) using the Becke3-LYP functional[24,25] and the 6-31G* basis set. All calculations were performed with the Gaussian 94 suite of programs.[26] Critical points have been characterized by diagonalizing the Hessian matrices calculated for the optimized structures; transition structures have only one negative eigenvalue (first order saddle points) with the corresponding eigenvector involving the expected formation of the two new oxirane bonds, the cleavage of the O_4O_5 and C_6O_4 dioxirane bonds and the shortening of the O_5C_6 bond. The transition mode imaginary frequencies (cm^{-1}) of the TSs are reported in Table 2 and 4. The search for TSs was limited to concerted transition structures, i.e., only the restricted B3LYP method has been used. However, Houk *et al.* have recently demonstrated that transition structures at the unrestricted B3LYP level are very similar to those at the restricted B3LYP level in the case of dioxirane epoxidations of alkenes.[16] We have confirmed this conclusion by carrying out unrestricted B3LYP/6-31G* optimization of the syn,exo-**2a** TS (see Scheme 4): geometry and energy almost exactly reproduce those of the restricted B3LYP calculations.

In Table 3 and 5, in addition to some relevant bond lengths (forming bond lengths are reported in Scheme 4 and 5), the following angles are gathered:

i) the torsional angles (H-O-C_1-C_2 and O-C_1-C_2-C_3) necessary to describe rotations about the O-C_1 and C_1-C_2 bonds

ii) the X_1-$\hat{O}_4$-O_5 angle which allows one to evaluate the alignment of the axis of the π cloud with the breaking O_4---O_5 bond (X_1 is a dummy atom placed at the center of the C_2-C_3 bond)

iii)|180° - α| (with α being the dihedral angle between the mean planes C_1-C_2-C_3-H_c and H_a-C_2-C_3-H_b, Scheme 2), which reflects distortion out of planarity of the olefinic moiety

iv) β and β' (Scheme 2), i.e., the dihedral angles between the forming oxirane plane and the mean planes C_1-C_2-C_3-H_c and H_a-C_2-C_3-H_b, respectively

v) γ, the angle between the attacking dioxirane plane ($C_6O_4O_5$) and the C=C bond axis. A value of 90° corresponds to an exact spiro structure while a value larger (smaller) than 90° means that the dioxirane plane is tilted away from (toward) the CH_2OH group.[27]

In order to produce theoretical activation parameters, vibrational frequencies in the harmonic approximation were calculated for all the optimized B3LYP/6-31G* structures and used, unscaled,[28] to compute the zero point energies, their thermal corrections, the vibrational entropies, and their contributions to activation enthalpies, entropies and free enthalpies (Table 6).

The contribution of solvent effects to the activation free enthalpy of the reactions under study are calculated via the self-consistent reaction field (SCRF) using the Tomasi model (interlocking spheres) by single point calculations (i.e., with unrelaxed gas-phase geometries of reactants and TSs) at the B3LYP/6-31G* level (Table 7).[29-32] Cartesian coordinates of all TSs are available on request.

RESULTS

First we investigated the conformational profile of 2-propen-1-ol and our results show that it closely parallels that of 3-buten-2-ol studied by Hehre at the HF/3-21G level.[33] Five minima were located on the conformational potential energy surface, i.e., **1a-e** (Scheme 3 and Table 1). Two of them (i.e., **1a** and **1b**) have almost the same energy and are definitely more stable than the other three (**1c**, **1d**, **1e**) so that they should be, by far, the most populated conformers.

In the most stable conformer **1b** the C-O bond approximately eclipses the CC double bond while the other conformer of similar stability, i.e. **1a**, features eclipsing between a C-H bond and the double bond. The hydroxylic hydrogen points toward the double bond in both these conformers thus suggesting the presence of a weak hydrogen bonding interaction between the OH group and the π bond.[34, 35] Consistently, the calculated OH stretching frequency in **1a** (ν_{OH} = 3733 cm^{-1}) and **1b** (ν_{OH} = 3731 cm^{-1}) is slightly lower than that of **1c** (ν_{OH} = 3747 cm^{-1}). Propenol conformers **1a**, **1c** and **1d** exhibit similar $OC_1C_2C_3$ angles and differ each other only for the hydroxylic hydrogen orientation (Scheme 3 and Table 1).

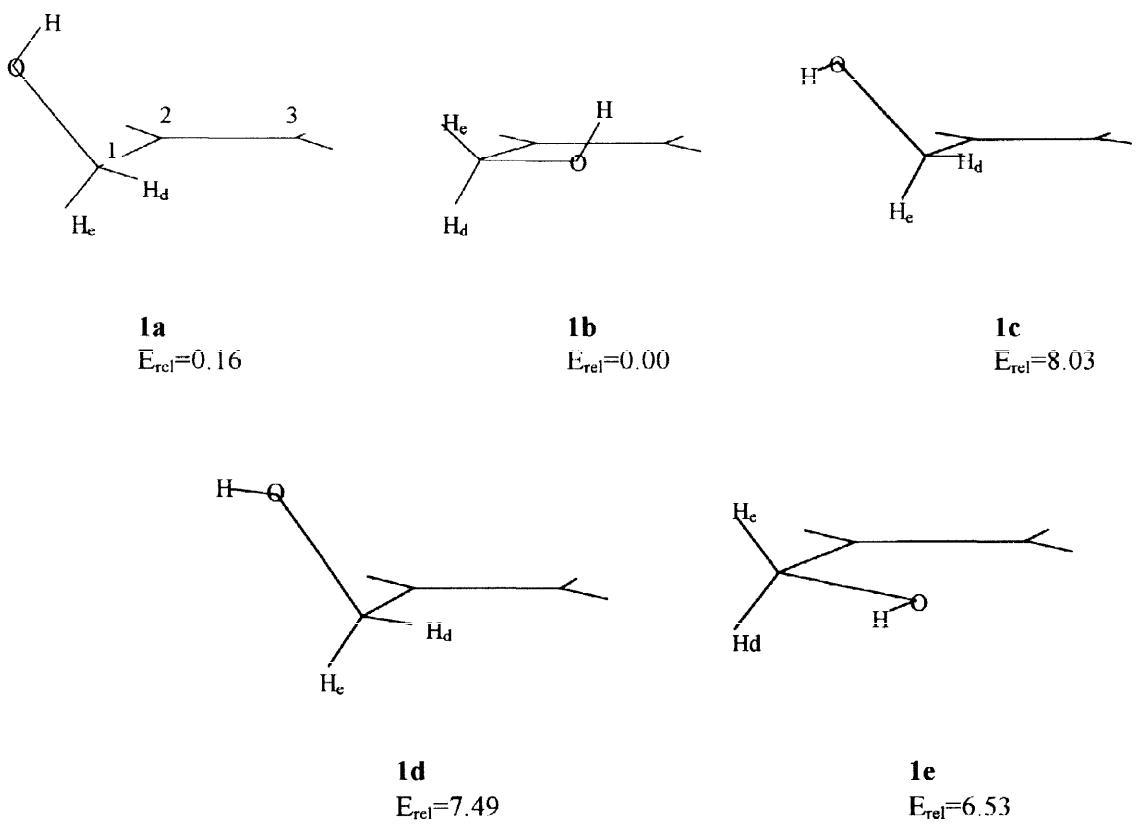

1a E_{rel}=0.16

1b E_{rel}=0.00

1c E_{rel}=8.03

1d E_{rel}=7.49

1e E_{rel}=6.53

Scheme 3. B3LYP Conformational minima of 2-propen-1-ol and their relative energies.

Table 1. Electronic energies (E), relative electronic energies (E_{rel}), dipole moment (μ), bond lengths (angstroms) and angles (degrees) of 2-propen-1-ol conformers, i.e., **1a-e**.

Conformer	E (hartree)	E_{rel} (kJ/mol)	μ (Debye)	O-H	HOC_1C_2	$OC_1C_2C_3$
1a	-193.110842	0.16	1.59	0.970	-57.4	123.6
1b	-193.110903	0.00	1.56	0.971	59.9	7.8
1c	-193.107845	8.03	1.64	0.969	170.9	129.3
1d	-193.108045	7.49	1.68	0.970	63.8	120.9
1e	-193.108419	6.53	1.79	0.968	-179.2	0.4

In both **1a** and **1b** the hydroxylic hydrogen is properly oriented to be involved, without a deep molecular structure reorganization, in hydrogen bonding with the dioxirane proximal oxygen from the very beginning of a spiro-exo attack.

In the other three conformers the hydroxylic hydrogen points away from the double bond. Their relative instability is attributable both to the absence of the stabilizing hydrogen bonding interaction and to the repulsion between the electron cloud of the oxygen lone pairs and that of the double bond.

Transition structures of the reaction with DHD

Seven transition structures for the reaction of DHD are depicted in Scheme 4 (see also Tables 2 and 3). All of them exhibit the now well established spiro-butterfly array[16-18] of reacting centers, i.e., the plane of the dioxirane ring and the plane of the forming oxirane ring are almost perpendicular to each other. Inspection of Scheme 4 makes it apparent that all the TSs can be related to a ground state propenol conformer. Thus, the syn,exo-**2a**, anti,exo-**2a** and anti,endo-**2a** TSs can be described as deriving from conformer **1a**. For example, syn,exo-**2a** originates from a syn (with respect to OH group), exo (the hydrogens of the dioxirane moiety are on the opposite side with respect to CH_2OH group) attack.

We did not manage to find the syn,endo-**2a** transition structure, while both the endo and exo orientation in the anti attack, by DHD on **1a**, lead to a first order saddle point. It is quite evident that in syn attack on **1a** an endo orientation of DHD can not take advantage of hydrogen bonding. Moreover the endo,syn approach should experience strong steric repulsion, between the hydrogens of DHD and the CH_2OH group, which can be alleviated by rotation about C_1-C_2 bond leading the system eventually to collapse to anti,endo-**2a** TS. An alternative possibility is rotation of the dioxirane moiety with formation of syn,exo-**2a**.

We have previously demonstrated that the endo orientation in the reaction of DHD with propene is less stable by 1.0 kcal/mol than the corresponding exo one[17]: this observation is confirmed by the relative energies of anti,endo-**2a** and anti,endo-**2c**, respectively, in comparison to those of anti,exo-**2a** and anti,exo-**2c**. Given that the energy difference between exo and endo TSs is steric in origin it certainly increases on passing from DHD to DMD reaction: this is why we did not calculate endo TSs for the reaction of the latter dioxirane (see below).

Table 2. Electronic energies (E)[a], relative electronic energies (E_{rel}), electronic activation energies ($\Delta E^{\neq}$) [b], dipole moments (μ), transition mode imaginary frequencies, charge transfer and net atomic charges (CHELPG) of TSs for the DHD epoxidations.

Transition structure	E (hartree)	E_{rel} (kJ\mol)	$\Delta E^{\neq b}$ (kJ\mol)	μ (Debye)	transition mode (cm^{-1})	net charge transfer [c]	net atomic charges[d]	
							O_4	O_5
syn,exo-**2a**	-382.714102	0.00	32.26	4.73	410.0	-0.27	-0.27	-0.42
syn,exo-**2b**	-382.713456	1.67	34.14	4.54	409.7	-0.30	-0.30	-0.42
anti,exo-**2a**	-382.706478	20.00	52.30	4.95	455.9	-0.30	-0.29	-0.43
anti,exo-**2c**	-382.705077	23.68	48.12	3.69	444.8	-0.32	-0.31	-0.43
anti,exo-**2d**	-382.705197	23.39	48.32	4.13	439.1	-0.32	-0.30	-0.42
anti,endo-**2a**	-382.705073	23.72	55.98	4.93	460.4	-0.29	-0.28	-0.42
anti,endo-**2c**	-382.703226	23.53	52.93	4.44	449.8	-0.31	-0.30	-0.41

[a]DHD: E = -189.615552 hartree, μ = 2.53 D [b]Calculated with respect to the corresponding ground state propenol conformer
[c]From propenol to DHD [d]Net atomic charge on DHD oxygens =-0.21

As quoted above the lower energy of conformer **1a** (by *ca.* 7.5 kJ/mol) than that of both **1c** and **1d** can be traced back to OH--π hydrogen bonding (in the former) and the lone pair-π bond repulsion (in the latters). Both these effects should be reduced as a result of the electrophilic attack on the double bond by DHD so that one would have expected a decrease in the favor of anti,exo-**2a** over anti,exo-**2c** and anti,exo-**2d**. This is what has been observed: anti,exo-**2a** is more stable than both anti,exo-**2c** and anti,exo-**2d** by only *ca.* 3.8 kJ/mol.

All of the transition structures **2** are characterized by low asynchrony in C----O bond formation. They also feature a pronounced O--O bond breaking while shortening of the C_6---O_5 bond and lengthening of the C_6-O_4 bond are underway even if less advanced. These observations, as well as the characteristics of the transition

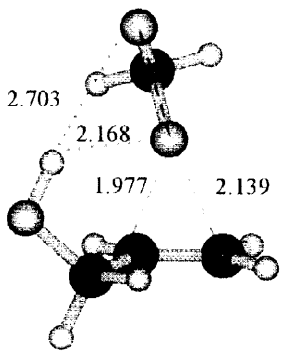

syn,exo-**2a**

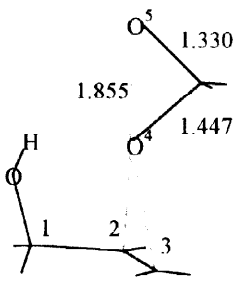

syn,exo-**2a** (side view)

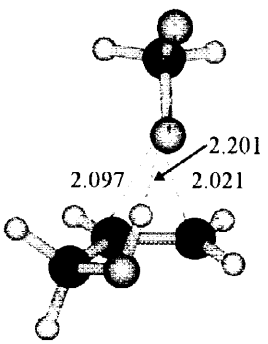

syn,exo-**2b**

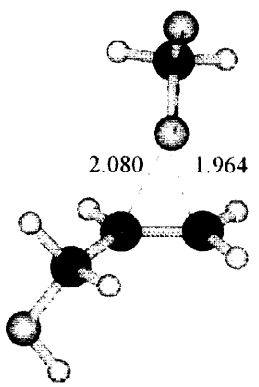

anti,exo-**2a**

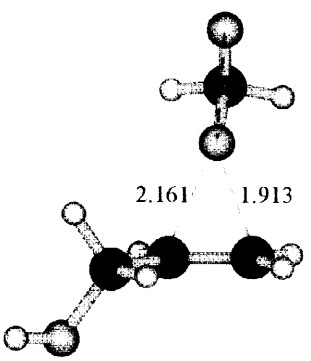

anti,exo-**2c**

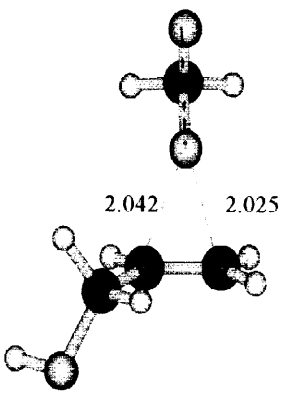

anti,exo-**2d**

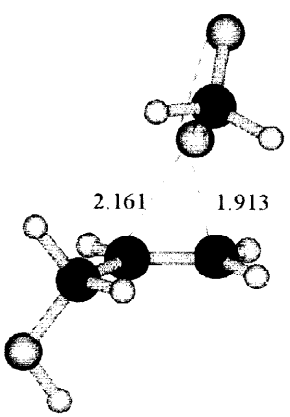

anti,endo-**2a**

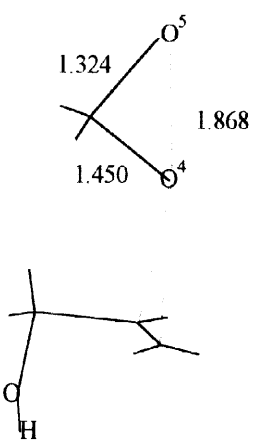

anti,endo-**2a** (side view)

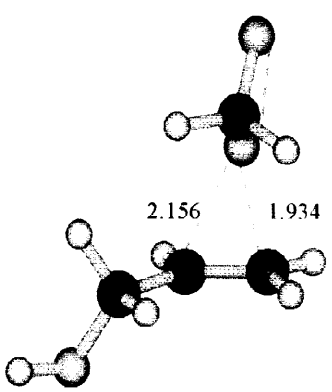

anti,endo-**2c**

Scheme 4. TSs for the reactions of DHD with propenol. Bond lengths in Å.

Table 3. Geometrical parameters[a, b] (bond lengths in Å, angles in degrees) of the TSs for the DHD epoxidations.

Parameter	syn,exo-**2a**	syn,exo-**2b**	anti,exo-**2a**	anti,exo-**2d**	anti,exo-**2c**	anti,endo-**2a**	anti,endo-**2c**
C_2C_3	1.371	1.370	1.372	1.371	1.370	1.372	1.372
O_4O_5	1.855	1.866	1.873	1.869	1.872	1.868	1.869
O_4C_6	1.447	1.449	1.453	1.450	1.451	1.450	1.449
C_6O_5	1.330	1.326	1.323	1.324	1.324	1.324	1.324
OH	0.975	0.974	0.971	0.970	0.970	0.970	0.971
HOC_1C2	-56.4	60.3	66.6	-79.2	-166.2	63.8	-163.7
$OC_1C_2C_3$	135.9	19.5	-118.4	-111.8	-121.8	-121.1	-122.9
$H_dC_1C_2C_3$	10.8	-99.4	6.6	5.9	0.3	3.5	-0.9
$X_1\hat{O}_4O_5$		168.4	164.8		165.8	166.3	166.4
$\|180-\alpha\|$	4.3	4.6	6.9	6.1	5.9	8.4	7.1
β	87.9	86. 7	88.6	88.5	89.3	97.3	96.0
β'	96.3	97.5	96.2	94.5	95.0	89.5	90.7
γ	72.4	91.6	95.7	91.8	93.8	104.1	102.5

[a]DHD ground state bond lengths: O_4O_5 = 1.506 Å, O_4C_6 = 1.353 Å. [b]Acetone ground state C=O bond length: 1.215 Å.

vector, clearly suggest that these TSs will collapse directly to final epoxide without prior formation of an intermediate such as a diradical.

A diradical intermediate has recently been advanced by Minisci and coworkers[36] on the basis of circumstantial experimental evidence in the context of an interesting mechanistic proposal for dioxirane epoxidation of alkenes. These authors emphasize, in a hot debate with other researchers,[37] the possible role of a radical pathway even if they also underline the difficulty to unambiguously discriminate between the concerted and stepwise mechanism.

To date, all the reported calculations, in particular restricted and unrestricted B3LYP calculations, do not provide support for the presence of biradical intermediates in dioxirane epoxidation of alkyl substituted alkenes.

Other aspects of dioxirane epoxidations will be discussed in the following section.

Transition structures of the reaction with DMD

Electron attracting effect of the OH group

TS structures of the reaction of DMD closely resemble those of DHD reaction and, in particular, also in the case of DMD there is a nice correspondence between geometries of TSs and those of propenol ground state conformers.

On the basis of TSs located for the DHD reaction we decided to limit our TS search to the chemically more significant TSs, i.e., to the two syn,exo TSs and to two anti,exo TSs (the most stable one and that one in which the hydroxylic hydrogen is antiperiplanar to the C_1C_2 bond). The transition structure geometries are reported in Scheme 5 (see also Tables 4 and 5).

We start our discussion from anti,exo-**3a**. On passing from **1a** to this TS there is a small clockwise rotation about the C_1-C_2 bond while the hydroxylic hydrogen still points toward the double bond. In anti,exo-**3a** there is not any possibility of hydrogen bonding so that its geometry and activation energy can profitably be compared to that of the exo TS from the reaction of DMD with propene (i.e., **4**, reported for comparison) in order to find out what are the differences induced by the presence of an allylic electron-withdrawing group. The dioxirane ring is almost exactly perpendicular to the C=C bond axis (γ = 93.5° in anti,exo-**3a** *vs* γ = 96.8° in **4**) with small tilting away from the CH_2OH group. The asynchrony in C---O bond formation is small and it is smaller than that in the epoxidation of propene (difference in forming bond lengths Δ = 0.07 Å in anti,exo-**3a** *vs* Δ = 0.15 Å in **4**; in both TSs the incipient C---O bond next to the CH_2X group is longer than the other) and the average incipient bond C---O length is similar. As asynchrony in bond formation in anti,exo-**3a** and **4** must be mostly the result of double bond polarization our results suggest that the double bond of propenol is slightly less polarized than that of propene.

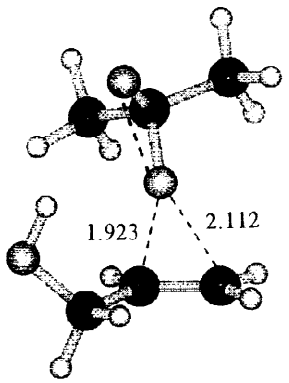

syn,exo-**3a**

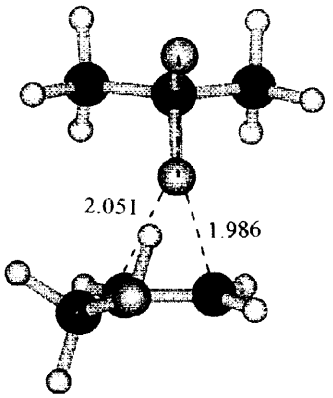

syn,exo-**3b**

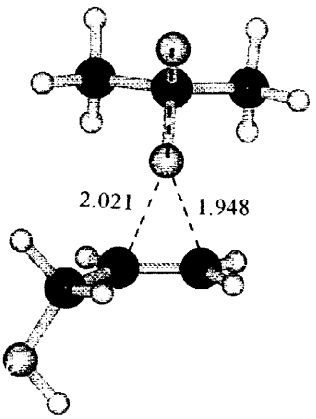

anti,exo-**3a**

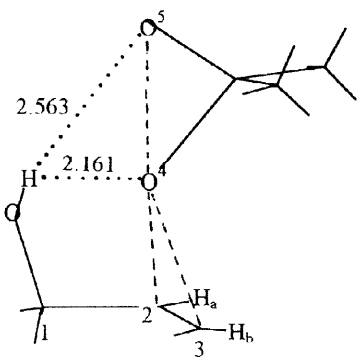

syn,exo-**3a** (side view)

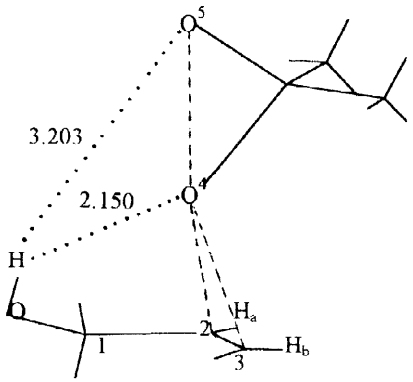

syn,exo-**3b** (side view)

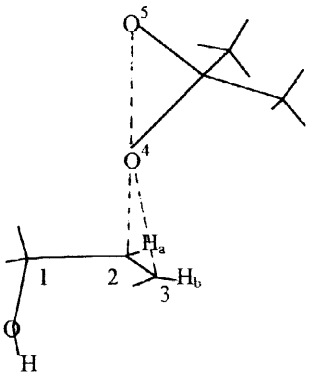

anti,exo-**3a** (side view)

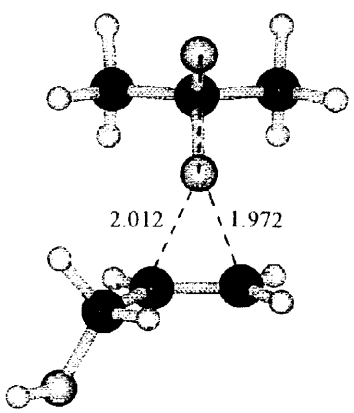

anti,exo-**3c**

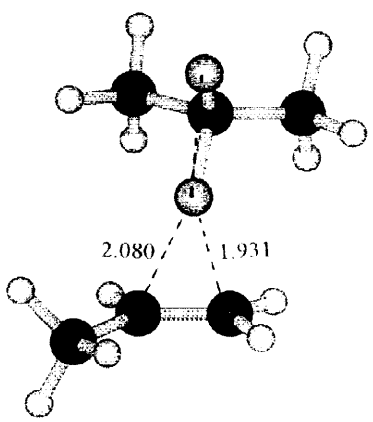

4

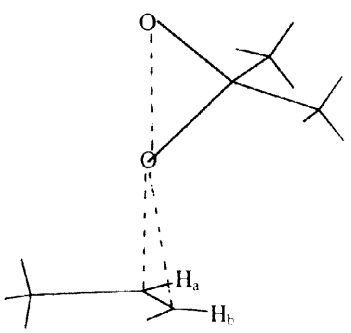

4 (side view)

Scheme 5. TSs for the reactions of DMD with propene (**4**) and propenol (syn,exo-**3a**, syn,exo-**3b**, anti,exo-**3a** and anti,exo-**c**). Bond lengths in Å.

Table 4. Electronic energies (E)[a], relative electronic energies (E_{rel}), electronic activation energies ($\Delta E^{\neq}$)[b], dipole moments (μ), transition mode imaginary frequencies, charge transfer and net atomic charges (CHELPG) of the TSs for the DMD epoxidations.

Transition structure	E (hartree)	E_{rel} (kJ\mol)	$\Delta E^{\neq b}$ (kJ\mol)	μ (Debye)	transition mode (cm^{-1})	net charge transfer[c]	net atomic charges[d] O_4	O_5
syn,exo-**3a**	-461.361074	0.00	49.12	4.51	479.1	-0.29	-0.30	-0.49
syn,exo-**3b**	-461.359879	3.14	52.42	4.52	483.1	-0.32	-0.37	-0.51
anti,exo-**3a**	-461.352124	23.51	72.63	4.57	529.3	-0.32	-0.35	-0.50
anti,exo-**3c**	-461.350646	27.36	68.62	3.21	517.8	-0.33	-0.36	-0.50
4	-386.151167		66.53	4.76	500.1	-0.29	-0.30	-0.51

[a]DMD: E = -268.268944 hartree, μ = 2.89 D [b]Calculated with respect to the corresponding ground state propenol conformer [c]From propenol to DMD [d]Net atomic charge on DMD oxygens = -0.26

Table 5. Geometrical parameters[a] (bond lengths in angstroms, angles in degrees) of the TSs for the DMD epoxidations.

Parameter	syn,exo-**3a**	syn,exo-**3b**	anti,exo-**3a**	anti,exo-**3c**	**4**
C_2C_3	1.374	1.374	1.376	1.374	1.375
O_4O_5	1.868	1.885	1.888	1.887	1.880
O_4C_6	1.497	1.502	1.509	1.506	1.495
C_6O_5	1.332	1.324	1.322	1.322	1.320
OH	0.976	0.976	0.970	0.970	
HOC_1C2	-57.4	58.3	66.6	-167.4	
$OC_1C_2C_3$	135.9	20.8	-114.5	-115.5	
$H_dC_1C_2C_3$	11.0	145.9	10.3	6.5	
$X_1\hat{O}_4O_5$	168.7	174.5	172.3	172.2	171.8
$\lvert 180-\alpha \rvert$	5.4	5.0	7.6	6.8	6.8
β	87.4	86.8	91.0	89.7	92.0
β'	97.6	98.1	95.6	96.5	96.0
γ	70.5	92.1	93.5	91.9	96.8

[a]DMD ground state bond lengths: O_4O_5 = 1.505 Å, O_4C_6 = 1.403Å.

The side views of anti,exo-**3a** and **4** illustrate other geometry details. The forming oxirane plane is slightly inclined toward the CH_2OH group, i.e, β (91.0° in anti,exo-**3a** *vs* 92.0°in **4**) is smaller than β' (95.6°in anti,exo-**3a** *vs* 96.0°in **4**), in order to alleviate the steric interaction between the methyl groups of the dioxirane moiety and the olefinic hydrogens (i.e., H_a and H_b).

The breakdown of the O---O bond is the dominant change observed in the dioxirane geometry on going from reactants to TS (Table 5). The O----O bond, while substantially assuming an orientation with respect to the π bond which is reminiscent of an S_N2-like reaction array, is not perfectly aligned to the π bond axis ($X_1\hat{O}_4O_5$ *ca.* 172° both in anti,exo-**3a** and **4**, X_1 is a dummy atom placed at the center of C_2C_3 bond). The latter features as well as the small out-plane deformation of the olefinic moiety ($\lvert 180°-\alpha \rvert$ = 7.6°in anti,exo-**3a** and 6.8° in **4**, the α angle is defined in Scheme 2) seem to be an inherent characteristic of transition structures of dioxirane epoxidation of alkenes as they are present in all the TSs calculated by us.

The above observations demonstrate that, as far as geometry is concerned, there are not any dramatic difference in anti,exo-**3a**, induced by the presence of the OH group, with respect to **4**.

Given the electrophilic nature of dioxirane attack on double bonds one can anticipate that there should be a larger electron density transfer from olefin to DMD in the case of **4** than in the case of anti,exo-**3a** and that there should be a decrease in reactivity, as far as electronic factors are concerned, on going from attack of DMD on propene to give **4** to the anti attack of DMD on **1a** to give anti,exo-**3a**. The latter prediction is borne out by the calculated electronic activation energies: $\Delta E^{\neq}_{exo,anti\text{-}3a}$ (72.63 kJ mol^{-1}) is higher by about 6.3 kJ mol^{-1} than $\Delta E^{\neq}_4$

(66.53 kJ mol^{-1}). However, calculated CHELPG[38] atomic net charges (as well as Mulliken charges)[39] do not provide any evidence that electron transfer is higher in **4** than in anti,exo-**3a**: actually the predicted charge transfer as well as the atomic net charges on the peroxy oxygens are similar in the two TSs (Table 4).

Smerz and Adam suggested that introduction of a methyl group on the double bond should induce a higher electron density transfer from olefin to dioxirane as well as a more pronounced polarization and heterolysis of the dioxirane peroxide bond. Our previous results on dioxirane epoxidation of ethene, propene and 2-butenes[17] as well as all transition structures reported here are in striking contrast to this statement. In fact, calculations clearly indicate that both the electron density transfer and the breakdown of the O----O bond do not change appreciably as a result of a relatively small variation of double bond nucleophilicity, i.e., for example, on passing from ethene to cis and trans 2-butenes or to propenol.

The observations reported above for exo,anti-**3a** also hold for exo,anti-**3c** (the latter is less stable than the former by 3.8 kJ mol^{-1}). For example conformation of **1c** is substantially retained during the anti approach to it by DMD and, in particular, the hydroxylic hydrogen keeps on being antiperiplanar with respect to the C_1-C_2 bond. The forming oxirane plane is slightly inclined toward the CH_2OH group (i.e., $\beta = 89.7°$ and $\beta' = 96.5°$) while the incipient C---O bond next to the CH_2OH group is longer than the other ($\Delta = 0.04$ Å). The rate retarding effect of the OH group is smaller ($\Delta E^{\neq} = 68.62$ kJ mol^{-1}) than in anti,exo-**3a**.

In summary, calculations suggest that the hyperconjugative (the C_1-O bond is almost parallel to the π cloud, i.e. it features an ideal orientation for an efficient σ_{co}^*-π interaction) and inductive electron attracting effect of the hydroxy group give rise to relatively small rate retarding effect.

Hydrogen bonding interaction

The other two TSs located in our study, i.e., syn,exo-**3a** and syn,exo-**3b** (Scheme 5), can be considered derived from the attack of DMD on the syn (with respect to OH) face of **1a** and **1b**, respectively, and show a potential energy much lower (by *ca.* 25.10 kJ mol^{-1}) than that of the anti TSs.

Formation of spiro-exo **3b** is accompanied by a small anticlockwise rotation about the C_1C_2 bond while the orientation of the hydroxylic hydrogen does not appreciably change. As in the anti TSs described above, also in this TS asynchrony in bond formation is very small ($\Delta = 0.065$ Å, once again with the C---O bond next to CH_2OH group longer than the other), the plane of the dioxirane part is almost perpendicular ($\gamma = 92.1°$) to the C=C bond axis and the forming oxirane plane is inclined toward the CH_2OH group [$\beta = 86.8°$ *vs* $\beta' = 98.1°$].

It is quite clear that the only underlying reason that can explain the lower potential energy of syn,exo-**3b** in comparison to that of the anti,exo TSs is hydrogen bonding. A convincing evidence in favor of an hydrogen bonding interaction can be found in the calculated O-H stretching frequency. O-H frequencies in syn TSs are sizable lower than those ones of the corresponding conformer of propenol (by *ca.* 50 cm^{-1} in syn,exo-**3b** and by *ca.* 80 cm^{-1} in syn,exo-**3a**), while in anti TSs there is not any deviation from the olefin frequency value (3734 cm^{-1} in anti,exo-**3a**, 3751 cm^{-1} in anti,exo-**3b**). One can consider also the fact that in syn,exo-**3b** the C_1-O bond is nearly coplanar with the C=C bond so that its destabilizing hyperconjugative electron withdrawing effect is certainly lower than in anti,exo-**3a** and anti,exo-**3c**. However, this effect (see above) can hardly account for more than *ca.* 2.5-6.3 kJ mol^{-1}. TS geometry also indicates that hydrogen bonding should involve the proximal O_4 more than the distal O_5. The latter oxygen has a larger negative net charge (-0.51) but is much more far away (3.20 Å) from the hydroxylic hydrogen than the former oxygen (2.15 Å) which also bears a sizable negative charge (-0.37). The latter conclusion apparently stands in contrast with the qualitative model of intramolecular (see **C** in Figure 1) hydrogen bonding proposed so far by researchers which suggests the preferential involvement of the dioxirane distal oxygen atom.[13]

However, one can argue that unsaturated cyclic alcohols[11,13] are prevented from assuming a conformation (for the CH_2OH moiety) similar to that present in syn,exo-**3b** and most of the experimental studies deal with this kind of alcohols. TS syn,exo-**3a** (the most stable of our TSs) is more adequate to provide an answer to the question whether O_5 can strongly be involved in hydrogen bonding or not . Actually it exhibits a conformation of the CH_2OH group that can be adopted also by unsaturated cyclic allylic alcohols without any added strain.

Hydrogen bonding in syn,exo-**3a** certainly involves both the oxygen atoms. Here again the distance between the hydroxylic hydrogen and the proximal O_4 (with -0.30 net charge) is lower (2.16 Å *vs* 2.56 Å) than that between the hydroxylic hydrogen and the distal O_5 (with -0.49 net charge). However, both distances are consistent with noticeable hydrogen bonding interaction.

From a geometrical standpoint in syn,exo-**3a** there is a pronounced asynchrony of the forming C----O bonds (Δ = 0.189 Å) that is unique with respect to all the other TSs described here. Even more, in contrast to all the other TSs, the shorter incipient C---O bond is that one next to the CH_2OH group. This "inverse" asynchrony in bond formation is accompanied by an "inverse" strong tilting of the dioxirane plane ($O_4C_6O_5$) toward the CH_2OH group. This plane is now far from being perpendicular to the C=C bond axis (γ = 73°). Both these deformations in an exo-spiro structure lead to a decrease in the H-----O_5 distance: the energy gain due to enhancement of hydrogen bonding interaction overcomes the energy loss which certainly accompanies these deformations.

Thus, geometry details of syn,exo-**3a**, while confirming that the overlooked OH------O_4 interaction plays a role in favoring the attack of dioxirane to both cyclic and acyclic allylic alcohols, also support previous hypothesis of the possible involvement of the distal O_5 in hydrogen bonding interactions.

Smerz and Adam stated that the $OC_1C_2C_3$ torsional angle is decisive for stereocontrol of dioxirane attack on the diastereotopic faces of allylic alcohols.[13] On the basis of PM3 conformational analysis of 2-cyclohexen-1-ol derivatives, they suggested a value of *ca.* 137-139° as the most favorable one for the association between the allylic hydroxy group and the dioxirane in the transition state. Transition structure syn,exo-**3a** with its $OC_1C_2C_3$ = 135.9° fully confirms their suggestion.

At this point one can ask whether the very same hydrogen bonding, observed in DMD epoxidation, involving the peroxide oxygens is present also in epoxidations of allylic alcohols by peroxyacids. Very recently Bach *et al*[40] located only two TSs for the reaction of propenol with peroxyformic acid. In both of them hydrogen bonding involves only the carbonyl moiety of the peroxyacid. We also investigated the same reaction and were able to locate five TSs in addition to those characterized by Bach *et al.* Geometries and energies of two of them provide support for the hypothesis that hydrogen bonding involving the peroxide moiety of the peroxyacid is operative. We will refer on these results in due course.

Activation free enthalpy of propenol vs propene epoxidation by DMD

Geometries of syn,exo-**3a-b** transition structures demonstrate that hydrogen bonding can be at work in the epoxidation of allylic alcohols by dioxiranes and that this stabilizing interaction leads to a substantial decrease in the potential energy of the system (by ≥ 25 kJ mol^{-1} in syn,exo-**3a**, syn,exo-**3b** *vs* anti,exo-**3c** and anti,exo-**3a**). Hydrogen bonding, present in syn attacks, gives rise to more ordered TSs (syn,exo-**3a** and syn,exo-**3b**) and this is reflected in their lower entropy (by 17-21 J $mol^{-1}K^{-1}$, Table 6) with respect to anti TSs.

The propenol and propene epoxidations with DMD can be taken as reasonable computational models for acyclic allylic alcohols and related olefin whose DMD epoxidation rate has been measured. As a consequence it is of interest to compare their reaction rate constants (relative as well as absolute) in gas phase and solution predicted by calculations.

The computational reaction rate constant in the case of 2-propen-1-ol is given by: $k_{apparent} = n_{1a}k_{syn,exo\text{-}3a} + n_{1b}k_{syn,exo\text{-}3b} + n_{1a}k_{anti,exo\text{-}3a} + n_{1c}k_{anti,exo\text{-}3c} + \ldots$ (n is the molar fraction of the propenol conformer and k its reaction rate constant via the indicated TS[41]). In fact equilibration between propenol conformers is certainly very fast, relative to epoxidation rate,[42] so that we are in the presence of a Curtin-Hammet system.[45]

The apparent gas phase reaction rate constant thus evaluated (neglecting other reaction pathways which give a negligible contribute to reaction rate) is: $k_{app.}$ = 1.3 10^{-4} L^{-1} mol s^{-1} at 298 K corresponding to $\Delta G^{\neq}_{app.}$ = 95.19 kJ mol^{-1}. This means that propenol is predicted by calculations much more reactive than propene ($\Delta G^{\neq}_{app.}$ = 104.14 kJ mol^{-1} and $k_{app.}$ = 3.5 10^{-6} L^{-1} mol s^{-1} at 298 K)[17] in striking contrast to the experimental results by Baumstark *et al.*[10] and Murray *et al.*[9] which indicate an enhancement in reactivity (*ca.* twice) on passing from allylic alcohols (e.g., 3-methyl-1-penten-3-ol: $\Delta G^{\neq}$ = 84.14 kJ mol^{-1} and k = 8.9 ± 0.4 10^{-3} L mol^{-1} s^{-1} at 296 K)

Table 6. Electronic activation energies($\Delta E^{\neq}$)[a], computed kinetic contributions to the thermodynamic properties[b] relative free enthalpy (G_{rel}) and calculated activation parameter[c] (at 298K) for the gas phase DMD epoxidations.

Structure	$\Delta E^{\neq a}$	ZPE[b]	δH^b	S^b	δG^b	G_{rel}	$\Delta H^{\neq a,c}$	$\Delta S^{\neq a,c}$	$\Delta G^{\neq a,c}$
1a		224.26	239.66	290.41	153.05	0.00			
1b		224.30	239.41	287.23	153.76	0.54			
1c		223.13	238.86	292.84	151.54	6.36			
DMD		232.96	250.16	300.49	160.54				
TS									
syn,exo-**3a**	49.12	460.95	491.41	414.93	367.69	0.00	53.18	-141.08	95.31
syn,exo-**3b**	52.42	459.70	490.74	422.79	364.68	0.12	56.07	-130.04	94.89
anti,exo-**3a**	72.63	458.15	490.28	436.81	360.03	15.86	75.56	-119.20	111.17
anti,exo-**3c**	68.62	457.06	489.65	440.78	358.23	17.91	71.71	-117.65	106.86

[a]Evaluated with respect to the corresponding ground state propenol conformer.

[b]Harmonic approximation assumed; standard state (298K) of the fugacity scale (pure perfect gas at 1 atm); energies in kJ/mol and entropies in J/mol K; ZPE: zero point energy; δH, δG are the kinetic contributions to molar enthalpy and free enthalpy (to be added to electronic energy); S is the molar entropy; symmetry numbers used to calculate entropy are $\sigma = 2$ for dioxirane and $\sigma = 1$ for 2-propen-1-ol conformer and all of the transition structures

[c]Energies in kJ/mol, entropy in J/mol K; standard state (298K) of the molar concentration scale (gas in ideal mixture at 1 mol/L, P=1 atm); $\Delta H^{\neq}$, $\Delta G^{\neq}$ are the molar activation enthalpy and free enthalpy; $\Delta S^{\neq}$ is the molar activation entropy. For conversion from 1 atm standard state to 1 mol/L standard state (both for gas phase) the following contributions need to be added to standard enthalpy, free enthalpy and entropy, respectively: -RT, RT ln R'T, -R ln R'T - R, where R' (0.082) is the value of the R constant given in L atm/mol K. For a reaction with A + B = C stoichiometry at 298 K, the corrections for $\Delta H^{\neq}$, $\Delta G^{\neq}$ and $\Delta S^{\neq}$ (RT, -RT ln R'T, R lnR'T + R, respectively) amount to 2.47 and -7.95 kJ/mol and 34.89 J/mol K, respectively.

Table 7. Solvent effect (kJ/mol) on free enthalpy ($\delta G^{\neq}_{sol}$), activation free enthalpy ($\delta\Delta G^{\neq}_{sol}$) and comparison between the corrected theoretical [$\Delta G^{\neq}_{gas}$ and $\Delta G^{\neq}_{sol}$ (apparent) at 298 K] and experimental ($\Delta G^{\neq}_{exp}$, at 296 K) data for DMD epoxidations.

TS	$\Delta G_{gas}^{\neq}$	$\Delta G_{gas}^{\neq}$ (apparent)	$\delta G^{\neq}_{sol}$[a,b]	$G^{\neq}_{sol,rel}$	$\delta\Delta G^{\neq}_{sol}$	$\Delta G^{\neq}_{sol}$[c]	$\Delta G^{\neq}_{sol}$ (apparent)	$\Delta G^{\neq}_{exp}$
syn,exo-**3a**	95.31		-41.42	2.72	-7.41	87.91		
syn,exo-**3b**	94.89	95.18	-44.27	0.00	-10.00	84.89	86.32	84.14
anti,exo-**3a**	111.17		-54.06	5.94	-20.04	91.13		
anti,exo-**3c**	106.86		-50.46	11.59	-15.15	91.71		
4	104.31	104.14[d]	-42.38		-25.23	79.08	78.95[d]	82.51

[a]Electrostatic solvent effect according to Tomasi model (acetone, ε = 21) at the B3LYP/6-31G* level of theory; $\delta G^{\neq}_{sol} = G^{\neq}_{sol} - G^{\neq}_{gas}$

[b] **1a**, **1b**, and **1c**: δG_{sol} = -17.11, -16.86 and -18.16, respectively; $G_{sol,rel}$ = 0.00, 0.79, 5.31, respectively; propene: δG_{sol} = -3.47; DMD: δG_{sol} = -17.15.

[c] $\Delta G^{\neq}_{sol}$ includes the $\delta\Delta G^{\neq}_{sol}$ correction ($\Delta G^{\neq}_{sol} = \Delta G^{\neq} + \delta\Delta G^{\neq}_{sol}$).

[d]It includes contribution of endo TS.

to the corresponding alkenes (e.g., 3-methyl-1-pentene: $\Delta G^{\neq}$ = 82.51 kJ mol^{-1} and k = 17.4 ± 0.4 10^{-3} L mol^{-1} s^{-1} at 296 K), however in acetone solution.

Given that B3LYP calculations seem to perform quite well in reproducing relative reactivity in dioxirane epoxidation,[17] we suggest that this dramatic reversal in relative reactivity on passing from computation to experiment should be attributed to solvation effects.

In fact, it is quite evident that the DMD (μ = 2.89 D) epoxidation of propene (μ = 0.36 D) should take advantage from a strong solvation of the polar transition state (i.e., **4**, μ = 4.76 D) which overcomes that of reactants. This reasoning is supported by introduction of electrostatic solvation effects through the Tomasi model by single point calculations: a remarkable decrease in activation free enthalpy of DMD epoxidation of propene ($\delta\Delta G^{\neq}_{sol}$ = 25.2 kJ mol^{-1}, in acetone, Table 7)[17] is observed.

In the case of propenol epoxidation solvation effects on activation free enthalpies should be less pronounced because also propenol conformers are significantly stabilized by solvation. In fact, solvent

stabilization of TSs with respect to reactants ($\delta\Delta G^{\neq}_{sol}$, Table 7) are 15.1-20.1 kJ mol^{-1} for the anti TSs and 7.5-10.0 kJ mol^{-1} for the syn TSs. This means that on the basis of activation free enthalpies corrected for electrostatic solvation effects propene should be oxidized by DMD faster ($\Delta G^{\neq}_{app.}$ = 78.95 kJ mol^{-1} and $k_{app.}$ = 9.1 10^{-2} L mol^{-1} s^{-1} at 298 K) than propenol ($\Delta G^{\neq}_{app.}$ = 86.31 kJ mol^{-1} and $k_{app.}$ = 4.7 10^{-3} L^{-1} mol s^{-1} at 298 K) in acetone solution. Even a very crude evaluation of solvation effects seems to substantially reconcile computational results on relative reactivity of allylic alcohols vs related alkenes with experimental data.

CONCLUSION

DFT calculations (B3LYP/6-31G* method) provide compelling evidence that stabilizing hydrogen bonding interactions are possible in the epoxidation of allylic alcohols with dioxiranes. Both the oxygen atoms of the dioxirane are involved in these interactions: not only the distal oxygen but also the proximal one. Transition structures with hydrogen bonding interactions show potential energies which are lower by > 25 kJ mol^{-1} than that of TSs in which hydrogen bonding is absent while, consistently, entropies of the former TSs are lower than those of the latter ones.

Calculations indicate that the electron attracting effect of the allylic hydroxy group has a relative small rate retarding effect. A much higher reactivity of propenol with respect to propene in gas phase is predicted by calculations but introduction of electrostatic solvation effects (acetone, Tomasi model) leads to a reversal of reactivity in substantial agreement with experimental data.

Acknowledgment. Financial support from MURST and CNR is gratefully acknowledged.

REFERENCES AND NOTES

1. Curci, R.; Fiorentino, M.; Troisi, L.; Edwards, J. O.; Pater, R. H. *J. Org. Chem.* **1980**, *45*, 4758.
2. Murray, R. W; Jeyarama, R.; Mohan, L. *Tetrahedron Lett.* **1986**, *27*, *2335*.
3. Adam, W.; Curci, R.; Edwards, J.O. *Acc. Chem. Res.* **1989**, *22*, 205.
4. Curci, R.; Dinoi, A.; Rubino, M. F. *Pure Appl. Chem.* **1995**, *67*, 811.
5. Murray, R. W.; Chem. Rev. **1989**, *89*, 1187.
6. Adam, W.; Chan, Y. Y.; Cremer, D.; Gauss, J.; Scheutzow, D.; Schindler, M. *J. Org. Chem.* **1987**, 52, 2800.
7. Adam, W.; Hadjiarapoglou, L.; Bialas, J. *Chem. Ber.* **1991**, *124*, 2377.
8. Adam, W.; Hadjiarapoglou, L.; Bialas, J. *Topics in Current Chemistry* **1993**, *164*, 46.
9. Murray, R. W.; Daquan Gu J. *J. Chem. Soc. Perkin Trans. 2* **1993**, 2203.
10. Baumastark; A. L.; Vasquez, P.C. *J. Org. Chem.* **1988**, *53*, 3437.
11. Murray, R. W.; Singh, M.; Williams, B. L.; Moncrieff, H. M. *Tetrahedron Lett.* **1995**, *36*, 2437.
12. Murray, R. W.; Hong Gu *J. Phys. Org. Chem.* **1996**, *9*, 751
13. Adam, W.; Smerz, A. K *Tetrahedron* **1995**, *51*, 13039.
14. Adam, W.; Smerz, A. K. *J. Org. Chem.* **1996**, *61*, 3506.
15. Jenson, C.; Houk, K. N.; Jorgensen W. L. *J. Am. Chem. Soc.* **1997**, *119*, 12982.
16. Houk, K. N.; Liu, J.; DeMello, N. C.; Condroski, K. R. *J. Am. Chem. Soc.* **1997**, *119*, 10147.
17. Gandolfi, R.; Freccero, M.; Sarzi-Amadè, M.; R. Rastelli *Tetrahedron* **1998**, *54*, 6123.
18. Bach, R. D; Glukhovtsev, M. N.; Gonzales, C.; Marquez, M.; Estevez, C. M.; Baboul, A.G.; Schlegel, H. B. *J. Phys. Chem. A* **1997**, *101*, 6092.
19. Bach, R. D.; Andres, J. L.; Owensby, A. L.; Schlegel, H. B.; McDouall, J. J. W. *J. Am. Chem. Soc.* **1992**, *114*, 7207.

20. Kraka, E.; Konkoli, Z.; Cremer, D.; Fowler, J.; Schaefer III, H. F. *J. Am. Chem. Soc.* **1996**, *118*, 10595.
21. Gutbrod, R.; Schindler, R. N.; Kraka, E.; Konkoli, Z.; Cremer, D. *Chem. Phys. Lett.* **1996**, *252*, 221.
22. Singleton, D. A.; Merrigan, S. R.; Jian Liu; Houk, K. N. *J. Am. Chem. Soc.* **1997**, *119*, 3385
23. Miaskiewicz, K; Smith, D. A. *J. Am. Chem. Soc.* **1998**, *120*, 1872
24. Becke, A. D. *J. Chem. Phys.* **1993**, *98*, 1372.
25. Lee, C.; Yang, W.; Parr, R.G. *Phys. Rev. B* **1988**, *37*, 785.
26. Gaussian 94; Frisch, M. J.; Trucks, G. W.; Schlegel, H. B.; Gill, P. M. W.; Johnson, B. G.; Robb, M. A.; Cheeseman, J. R.; Keith, T.; Peterson, G. A.; Montgomery, J. A.; Raghavachari, K.;Al-Laham, M. A.; Zakrzewski, V. G.; Ortiz, J. V.; Foresman, J. B.; Cioslowski, J.; Stefanov, B. B.; Nanayakkara, A.; Challacombe, M.; Peng, C. Y.; Ayala, P. Y.; Chen, W.; Wong, M. W.; Andres, J. L.;Replogle, E. S.; Gompert, R, Martin, R. L.; Fox, D. J.; Binkley, J. S.; Defrees, D. J.; Baker, J.; Stewart, J. P.; Head-Gordon, M.; Gonzales C.; Pople, J. A. Gaussian, Inc.: Pittsburgh, PA, 1995.
27. Deviation from 90° may be the conseguence not only of dioxirane plane tilting but also of rotation of this plane about O_5-O_4 axis. The former effect is largely dominant in the reported structures.
28. Rastelli, A.; Bagatti, M.; Gandolfi, R. *J. Am. Chem. Soc.* **1995**, *117*, 4965.
29. Miertus, S.; Tomasi, J. *J. Chem. Phys.* **1982**, *65*, 2392.
30. Miertus, S.; Scrocco, E.; Tomasi, J. *J. Chem. Phys.* **1981**, *55*, 117.
31. Coitino, E. L.; Tomasi, J.; Ventura, O. N. *J. Chem. Soc. Faraday Trans.* **1994**, *90*, 1745.
32. Tomasi, J.; Persico, M. *Chem Rev.* **1997**, *94*, 2027.
33. Kahn, S. D.; Hehre,W. J. *Tetrahedron Lett.* **1985**, *26*, 3647.
34. Smith, S.; Carballo, N.; Wilson, E. B.; Marstokk, K. M.; Mollendal, H. *J. Am. Chem. Soc.* **1985**, *107*, 1951.
35.Morokuma, K.; Wipff, G. *Chem. Phys. Lett.* **1980**, *74*, 400.
36. Minisci, F.; Bravo, A.; Fontana, F.; Fronza, G.; Zhao L. *J. Org. Chem.* **1998**, *63*, 254.
37. Adam, W.; Curci, R.; D'Accolti, L.; Dinoi, A.; Fusco, C.; Gasparrini, F.; Kluge, R.; Paredes, R.; Schulz, M.; Smerz, A. K.; Veloza, L. A.; Weinkotz, S.; Winde, R. *Chem. Eur. J.* **1997**, *3*, 105.
38. Hehre, W. J.; Radom, L.; Schleyer, P. v.R.; Pople, J. A. *Ab initio molecular orbital theory* Wiley-Interscience **1986**, 25
39. Mulliken charge distribution in TSs **2** and **3** is similar to CHELPG one. For example, charge transfer from propenol to DMD, evaluated on the basis of Mulliken partition is -0.31 and -0.33 in syn,exo-**2a** and syn,exo-**2b**, respectively, vs -0.29 and -0.32 on the basis of CHELPG partition. Also atomic net charges on DMD oxygens are similar in the two methods (Mulliken vs CHELPG, respectively: on O_4: -0.37 *vs* -0.30 in syn,exo-**2a** and -0.38 *vs* -0.37 in syn,exo-**2b**; on O_5: -0.47 *vs* -0.49 in syn,exo-**2a** and -0.49 *vs* -0.51 in syn,exo-**2b**).
40. Bach, R. D.; Estévez, C. M.; Winter J. E.; Glukhovtsev, M.N. *J. Am. Chem. Soc.* **1998**, *120*, 680.
41. For sake of simplicity only the three conformations **1a**, **1b** and **1c** of propenol were considered for the evaluation of the absolute reaction rate ($k_{app.}$). Moreover, the individual k_i were calculated as follows: e.g., $\ln k_{exo,sin\text{-}3a}$ (gas phase) = $\ln(k_b/h) + \ln T - (\Delta G^{\neq}_{exo,sin\text{-}3a}/RT)$.
42. Barrier to rotations about Csp_3-Csp_3 as well as Csp_3-Csp_2 single bonds in simple derivatives are lower than 21-25 kJ mol^{-1}. For example in n-butane the highest energy conformation, that one which features eclipsing of the two methyl groups, is 21 kJ less stable than the lowest energy anti conformation.[43,44]
43. Eliel, E. L.; Wilen, S. H. *Stereochemistry of Carbon Compounds* Wiley, New York, 1994, Chapt. 10.
44. Allinger, N.L.; Grev, R.S.; Yates, B.F.; Schaefer III, H. F. *J. Am. Chem. Soc.* **1990**, *112*, 114.
45. Seeman, J. I. *Chem. Rev.* **1983**, *83*, 83.